

Entropy Changes in the Dissociation of Proton-Bound Complexes: A Variational RRKM Study[†]

Julie A. D. Grabowy and Paul M. Mayer*

Chemistry Department, University of Ottawa, Ottawa, Ontario, Canada

Received: April 13, 2004; In Final Form: July 27, 2004

Microcanonical variational transition state theory was employed to determine the entropy of activation, ΔS^\ddagger , for the dissociation of a series of acetonitrile–alcohol proton-bound pairs over an internal energy range corresponding to metastable ion decomposition observations on a magnetic sector mass spectrometer. It was found that ΔS^\ddagger decreases with increasing size of the alcohol chain in the complex. These values ranged from 64 to 75 J K⁻¹ mol⁻¹ for (CH₃CN)(CH₃OH)H⁺, 34–43 J K⁻¹ mol⁻¹ for (CH₃CN)(CH₃CH₂OH)H⁺, 6 J K⁻¹ mol⁻¹ for (CH₃CN)(CH₃CH₂CH₂OH)H⁺, and 11–13 J K⁻¹ mol⁻¹ for (CH₃CN)((CH₃)₂CHOH)H⁺. The entropy of activation was compared to the thermodynamic ΔS for the overall reaction, and larger relative changes are observed between ΔS^\ddagger values than for ΔS .

1. Introduction

Transition state theory (TST) can be used to determine the tightness or looseness of the transition state molecular configuration as compared to that of the reactants and hence the entropy of activation, ΔS^\ddagger . From the thermodynamic version of transition state theory, the Arrhenius pre-exponential factor A can be written in terms of ΔS^\ddagger ,

$$A = \frac{k_B T}{h} e^n e^{(\Delta S^\ddagger/R)} \quad (1)$$

where k_B is Boltzmann's constant, T is temperature, h is Planck's constant, n is the molecularity of the reaction ($n = 2$ for a bimolecular process), R is the gas constant, and ΔS^\ddagger is the entropy of activation. When it comes to a bond scission reaction in a gas-phase ion, ΔS^\ddagger can be measured directly from the temperature dependence of the dissociation. However, due to the large binding energies typical of gas-phase ions and the low pressures in mass spectrometers, it is difficult to sufficiently heat an ion to its dissociation threshold for kinetics measurements. Blackbody infrared dissociation (BIRD) is the only practical method for directly measuring the temperature dependence of ion decomposition.^{1,2} The entropy of activation for a bond cleavage reaction can also be obtained by fitting experimental dissociation versus internal energy data. Threshold photoelectron photoion coincidence (TPEPICO) $k(E)$ versus E data can be modeled directly with RRKM theory to extract ΔS^\ddagger .^{3,4} Threshold collision-induced dissociation (CID) or surface-induced dissociation (SID) experiments can also include ΔS^\ddagger in the modeling of ion dissociation curves.^{5,6} PEPICO studies, however, cannot be applied to even electron ions such as proton-bound pairs.

A third method, the so-called kinetic method, can be used for estimating ΔS^\ddagger in the dissociation of electrostatically bound complexes.⁷ This method is based on the rates of two competitive dissociation channels of mass-selected cluster ions and uses

tandem mass spectrometry to extract thermochemical information such as proton affinities. The original implementation of the kinetic method assumed that the ΔS^\ddagger values for the two competing channels were the same and thus their difference $\Delta(\Delta S^\ddagger) = 0$. In accordance with these assumptions, the following expression was derived:

$$\ln\left(\frac{k_1}{k_2}\right) = \frac{\text{PA}(B_1) - \text{PA}(B_2)}{RT_{\text{eff}}} \quad (2)$$

where $\text{PA}(B_1)$ and $\text{PA}(B_2)$ are the proton affinities of B_1 and B_2 , respectively, R is the gas constant, and T_{eff} is the effective temperature. To examine systems in which entropy effects did not cancel out, modifications were made to the original method^{8–12} so that $\Delta(\Delta S^\ddagger)$ could be obtained from experiments performed at different center-of-mass collision energies. Information about the individual dissociation channel ΔS^\ddagger values cannot be obtained with either the original or extended methods. Cooks and co-workers introduced an entropy-corrected version of the kinetic method¹³ in which the entropy term is explicitly rewritten as $\Delta(\Delta S^\ddagger)/R = \Delta S_2^\ddagger/R - \Delta S_1^\ddagger/R$, giving

$$\ln\left(\frac{k_1}{k_2}\right) - \frac{\Delta S_1}{R} = \frac{\text{PA}(B_1) - \text{PA}(B_2)}{RT_{\text{eff}}} + \frac{\Delta S_2}{R} \quad (3)$$

assuming that $\Delta(\Delta S)$, the relative reaction entropies, and $\Delta(\Delta S^\ddagger)$ are very similar. The (k_1/k_2) ratio for each pair of compounds is corrected by the entropy term of the reference base. This approach can be used to obtain ΔS_2^\ddagger provided the entropy effect for the competing reaction (ΔS_1^\ddagger) is known.

A fourth approach used in the determination of $\Delta(\Delta S^\ddagger)$ for proton-bound pairs is the method of kinetic energy release distributions (KERDs).¹⁴ This method, used in conjunction with finite heat bath theory analysis, allows relative proton affinities of monomeric species to be determined. To obtain $\Delta(\Delta S^\ddagger)$, experimental KERDs are first fit to yield transition state temperatures according to the equation $p(\epsilon) = e^l \exp(-\epsilon/k_B T^\ddagger)$ where ϵ is the kinetic energy release, l is a parameter experimentally fit to range between 0 and 1, k_B is Boltzmann's constant, and T^\ddagger is the transition state temperature defined by

[†] Part of the special issue "Tomas Baer Festschrift".

* To whom correspondence should be addressed. E-mail: pmayer@science.uottawa.ca.

the average kinetic energy passing through the transition state.¹⁵ The following equation is then used to determine $\Delta(\Delta S^\ddagger)$ from the experimental branching ratio and the two transition state temperatures:

$$\ln\left(\frac{k_1}{k_2}\right) = \frac{\Delta(\Delta S^\ddagger)}{k_B} + C \ln\left(\frac{T_1^\ddagger}{T_2^\ddagger}\right) \quad (4)$$

where k_1 and k_2 are the branching ratio for the two monomers, C is the heat capacity of the energized ion, k_B is Boltzmann's constant, and T_1^\ddagger and T_2^\ddagger are the transition state temperatures for the two reactions.

A central question arises when discussing ΔS^\ddagger for a bond cleavage reaction that has no reverse energy barrier and that is the location of the effective transition state. Since there is no saddle point, the rate constant will depend on the molecular configuration corresponding to the minimum sum-of-states along the reaction coordinate. It has been assumed that this variational transition state lies at large internuclear separations and thus $\Delta(\Delta S^\ddagger)$ is similar to $\Delta(\Delta S)$,^{8–13,16} where ΔS is the thermodynamic reaction entropy change for each of the two competing bond scission reactions. Ervin¹⁷ presented a rigorous analysis of the kinetic method using RRKM theory and placed the effective transition state at the centrifugal barrier to the dissociation, and thus $\Delta(\Delta S^\ddagger)$ was always greater than $\Delta(\Delta S)$ by a relatively small amount, $\sim 6 \text{ J K}^{-1} \text{ mol}^{-1}$. But again, only $\Delta(\Delta S^\ddagger)$ was investigated, not the ΔS^\ddagger for a single dissociation channel. Drahos and Vekey¹⁶ also assumed very late transition states in their modeling of the kinetic method (and thus $\Delta(\Delta S^\ddagger) = \Delta(\Delta S)$).

In this work, we wished to determine ΔS^\ddagger for a single dissociation channel explicitly and examine how it changes with molecular functionality and how it relates to ΔS for the reaction. Microcanonical variational transition state theory (μ -VTST) is used to model the unimolecular dissociation of a series of proton-bound acetonitrile–alcohol pairs $(\text{CH}_3\text{CN})(\text{XOH})\text{H}^+$ (where $\text{X} = \text{CH}_3, \text{CH}_3\text{CH}_2, \text{CH}_3\text{CH}_2\text{CH}_2,$ and $(\text{CH}_3)_2\text{CH}$) to extract the entropy of activation for the bond scission reactions. These proton-bound pairs have been shown to either dissociate by cleavage of the intracuster hydrogen bond or rearrange via an internal $\text{S}_{\text{N}}2$ reaction to lose water.¹⁸ Due to the increasing proton affinities (PAs) of the alcohols in going from methanol to 2-propanol, there is a change in the bond cleavage products from $\text{CH}_3\text{CNH}^+ + \text{CH}_3\text{OH}$ and $\text{CH}_3\text{CNH}^+ + \text{CH}_3\text{CH}_2\text{OH}$ to $\text{CH}_3\text{CNH}^+ + \text{CH}_3\text{CH}_2\text{CH}_2\text{OH}_2^+$ and $\text{CH}_3\text{CN} + (\text{CH}_3)_2\text{OH}_2^+$ since the PA of CH_3CN lies between that of ethanol and the propanols.

2. Computational Procedures

Ab initio molecular orbital calculations were carried out using the Gaussian 98 suite of programs.¹⁹ Geometries were optimized and harmonic vibrational frequencies were calculated, at the MP2/6-31+G(d) level of theory. All vibrational frequencies were scaled by the factor of 0.9434 recommended by Scott and Radom²⁰ prior to use.

Variational transition state theory was used to model the unimolecular dissociation of the proton-bound complex according to the following expression:^{21–24}

$$k(E) = \frac{\sigma N^\ddagger(E, E_0, R^*)}{h \rho(E)} \quad (5)$$

where $k(E)$ is the unimolecular rate constant at an ion internal energy, E , σ is the reaction symmetry number, h is Planck's

constant, E_0 is the 0 K activation energy, $\rho(E)$ is the reactant ion density of states, and $N^\ddagger(E, E_0, R^*)$ is the sum-of-states for the fragmentation bottleneck located at an intracuster separation R^* . The density and sum-of-states were calculated by the direct count method of Beyer and Swinehart.²⁵

The energy of each proton-bound pair ABH^+ was calculated for several intracuster separations, R (without optimization), ranging from the equilibrium value to 12 Å. An example is shown in Figure 1 for $(\text{CH}_3\text{CN})(\text{CH}_3\text{OH})\text{H}^+$ in which the OH bond length refers to the $\text{CH}_3\text{CNH}^+ \cdots \text{O}(\text{H})\text{CH}_3$ distance. The reaction path of a dissociation process does not have a reaction barrier, and so a unique transition state cannot be obtained with ab initio MO calculations. The transition state responsible for the simple bond cleavage of the proton-bound pair was therefore located by finding the intracuster separation, R^* , having the lowest sum-of-states and thus responsible for the minimum reaction flux. The normal modes of ABH^+ were assigned to frequencies of either one of the dissociation products AH^+ or B (common modes) or to one of the six modes that are converted to translational and rotational degrees of freedom of the products (the vanishing modes) by comparing their calculated atomic displacements. This process is straightforward since the six vanishing modes are the only ones in which all of the atoms in ABH^+ are displaced. For the common modes, the transition state frequencies were chosen to be the average of their values in the complex and in the free product and hence were the same for every configuration along the curve in Figure 1. Of the six vanishing modes, the lowest frequency mode was a torsion mode and was treated as a free rotor in the RRKM calculations²¹ while the highest frequency mode was the intracuster stretching frequency representing the reaction coordinate for the cleavage of the complex. The four remaining frequencies were then scaled according to the following equation:^{21,26,27}

$$\nu'(R) = \nu(R_{\text{eq}}) e^{-\alpha(R-R_{\text{eq}})} \quad (6)$$

where $\nu'(R)$ is the value of the frequency at an intracuster separation R , R_{eq} is the equilibrium hydrogen bond distance, and α is an adjustable parameter. This equation is based on the assumption that the four modes will vanish exponentially to zero along the reaction coordinate.^{26,27} The parameter α is adjustable and was determined by comparing the four vanishing frequencies of each molecular system with those calculated for the optimized $\text{AH}^+ \cdots \text{B}$ structures having intracuster separations of 5.0 and 8.0 Å. The value of α used to calculate the new frequencies at each R value was an average of the α values obtained at intracuster separations of 5.0 and 8.0 Å. The four α values derived for each of the four complexes as well as all vibrational frequencies used in the RRKM treatment are listed in Table 1. The logarithm of the sum-of-states, $\log(N^\ddagger)$, was then calculated as a function of R .

This approach to locating the minimum in N^\ddagger is, of course, only approximate. It is impossible to determine how approximate unless a fully optimized dissociation reaction coordinate is obtained (avoiding the use of eq 6). Even then, however, it is uncertain how accurately most modest computational levels of theory can model a dissociation reaction coordinate. In light of this fact, all computational approaches to this problem will yield only estimates of the true entropy of activation. By treating all of the systems in the same manner, it is hoped that at least the relative ΔS^\ddagger values will be reliable. We estimated the uncertainty in the ΔS^\ddagger values, using the spread in the α values obtained for the 5.0 and 8.0 Å geometries, to be $\pm 3 \text{ J K}^{-1} \text{ mol}^{-1}$.

According to statistical thermodynamics, the translational entropy (S_{trans}), rotational entropy (S_{rot}), and vibrational entropy

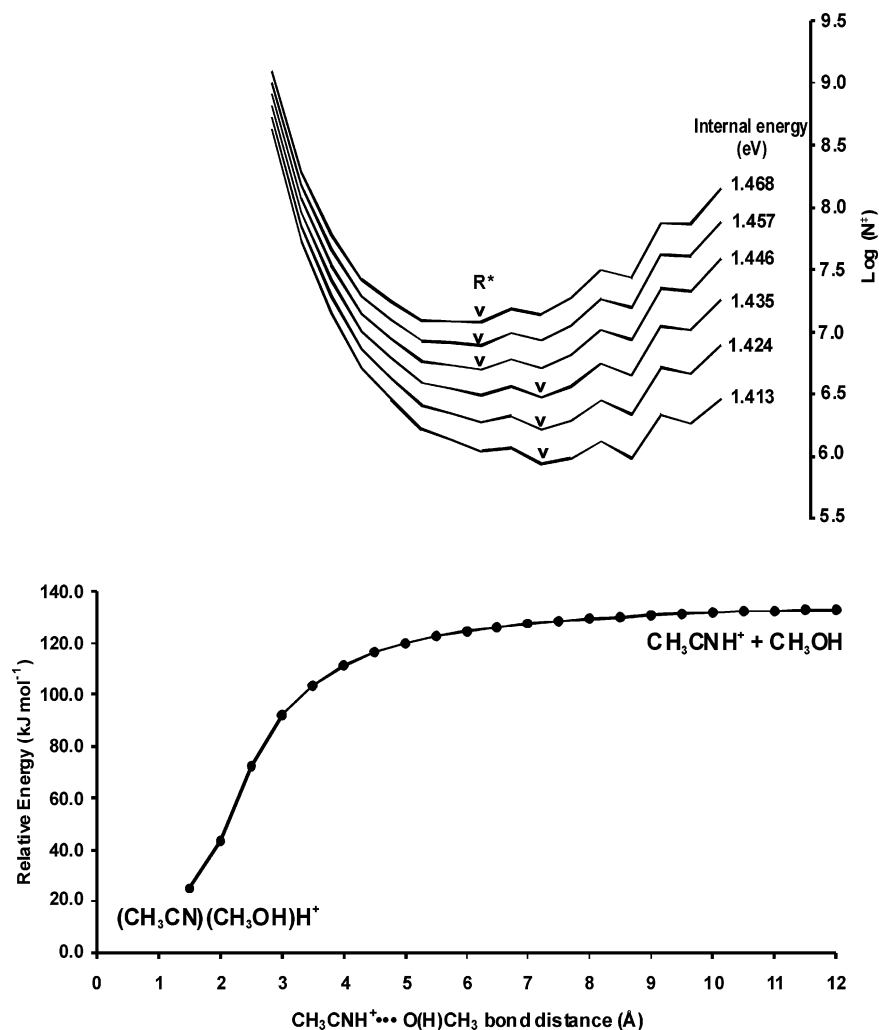


Figure 1. Plot of the relative energy vs hydrogen bond distance (R) in the $(\text{CH}_3\text{CN})(\text{CH}_3\text{OH})\text{H}^+$ complex at the MP2/6-31+G(d) level of theory. R refers to the $\text{CH}_3\text{CNH}^+\cdots\text{O}(\text{H})\text{CH}_3$ distance. Superimposed on the figure is the calculated sum-of-states, $\log(N^*)$, as a function of R at various internal energies and the locations, R^* , of the variational transition state.

(S_{vib}) of a nonlinear molecule in a canonical ensemble can be written as follows:

$$S_{\text{trans}} = \frac{5}{2}L_{\text{N}}k_{\text{B}} + L_{\text{N}}k_{\text{B}} \ln\left(\left(\frac{2\pi Mk_{\text{B}}T}{L_{\text{N}}h^2}\right)^{3/2} \left(\frac{k_{\text{B}}T}{P_0}\right)\right) \quad (7)$$

$$S_{\text{rot}} = \frac{3}{2}L_{\text{N}}k_{\text{B}} + L_{\text{N}}k_{\text{B}} \ln\left(\frac{\pi^{1/2}(8\pi^2k_{\text{B}}T)^{3/2}}{\sigma h^2} (I_{\text{A}}I_{\text{B}}I_{\text{C}})^{1/2}\right) \quad (8)$$

$$S_{\text{vib}} = L_{\text{N}}k_{\text{B}} \sum_{j=1}^{3n-6} \left(\frac{(hv_j/k_{\text{B}}T)e^{-hv_j/k_{\text{B}}T}}{1 - e^{-hv_j/k_{\text{B}}T}} - \ln(1 - e^{-hv_j/k_{\text{B}}T}) \right) \quad (9)$$

where L_{N} , k_{B} , and h are Avogadro's number, Boltzmann's constant, and Planck's constant, respectively; M is the molar mass; P_0 is 101 325 Pa; σ is the symmetry number; I_{A} , I_{B} , and I_{C} are the three principal moments of inertia; ν_j is the vibration frequency associated with the j th normal mode. All entropy values were calculated at 600 K.

3. Results and Discussion

The α values of the four disappearing modes were found to be unique (Table 1). If we consider the first bending mode, the α value is 0.46 \AA^{-1} for $(\text{CH}_3\text{CN})(\text{CH}_3\text{OH})\text{H}^+$ and

0.27 \AA^{-1} for $(\text{CH}_3\text{CN})(\text{CH}_3\text{CH}_2\text{OH})\text{H}^+$ and finally stabilizes to 0.13 \AA^{-1} for $(\text{CH}_3\text{CN})(\text{CH}_3\text{CH}_2\text{CH}_2\text{OH})\text{H}^+$ and $(\text{CH}_3\text{CN})((\text{CH}_3)_2\text{CHOH})\text{H}^+$. The four α values for $(\text{CH}_3\text{CN})(\text{CH}_3\text{OH})\text{H}^+$ range from 0.46 and 0.44 \AA^{-1} for the first and second modes to 0.20 \AA^{-1} for the third and fourth modes. For $(\text{CH}_3\text{CN})(\text{CH}_3\text{CH}_2\text{OH})\text{H}^+$, the α values were more consistent, averaging around 0.25 \AA^{-1} . The α values for $(\text{CH}_3\text{CN})(\text{CH}_3\text{CH}_2\text{CH}_2\text{OH})\text{H}^+$ and $(\text{CH}_3\text{CN})((\text{CH}_3)_2\text{CHOH})\text{H}^+$ were comparable to each other while being much smaller than the values obtained for the other two pairs. The α values obtained for the four disappearing modes in $(\text{CH}_3\text{CN})(\text{CH}_3\text{CH}_2\text{CH}_2\text{OH})\text{H}^+$ and $(\text{CH}_3\text{CN})((\text{CH}_3)_2\text{CHOH})\text{H}^+$ are more similar to those found in ion-radical dissociation reactions $((\text{CH}_3)_2\text{NH}_2^+ + \cdot\text{CH}_2\text{N}(\text{H})\text{CH}_3, \alpha = 0.08 \text{ \AA}^{-1})^{28}$ and ion-molecule reactions $(\text{Li}^+ + \text{H}_2\text{O}, \alpha = 0.1 \text{ \AA}^{-1})^{29}$. This would suggest that the acetonitrile-propanol proton-bound pairs contain more ionic character, while the larger α values observed with the methanol- and ethanol-containing pairs suggest more covalent character within the complex. This does not necessarily correlate with a stronger bond as the bond dissociation energies (calculated at the MP2/6-31+G(d) level of theory) are 129, 139, 132, and 127 kJ mol^{-1} for $\text{X} = \text{CH}_3, \text{CH}_3\text{CH}_2, \text{CH}_3\text{CH}_2\text{CH}_2,$ and $(\text{CH}_3)_2\text{CH}$, respectively. All values of α for the four complexes are much less than the α values found in bond scission reactions of neutral molecules

TABLE 1: Calculated Vibrational Frequencies for Proton-Bound Acetonitrile–Alcohol Pairs, Transition States, and Their Dissociation Products

	harmonic frequencies (cm ⁻¹) ^a
(CH ₃ CN)(CH ₃ OH)H ⁺	67, 80, 129, 147, 260, 329, 331, 517, 882, 908, 964, 1013, 1015, 1098, 1160, 1290, 1374, 1417, 1417, 1419, 1451, 1454, 1665, 1943, 2155, 2943, 2983, 3039, 3040, 3103, 3117, 3470
CH ₃ CNH ⁺	322, 322, 541, 541, 866, 1008, 1008, 1362, 1394, 1394, 2183, 2927, 3029, 3029, 3486
CH ₃ OH	313, 1004, 1028, 1129, 1306, 1437, 1464, 1473, 2908, 2977, 3045, 3562
transition state (common)	325, 327, 415, 711, 725, 984, 1010, 1011, 1063, 1209, 1233, 1265, 1368, 1405, 1406, 1428, 1459, 1462, 2169, 2714, 2935, 2946, 3034, 3034, 3047, 3074, 3516
transition state (vanishing) ^b	67, 80, 129, 147
α values	0.46, 0.44, 0.20, 0.20
rotational constant for rotor (GHz)	23.3
moment of inertia (10 ⁻⁴⁷ kg m ⁻²)	360, 643, 667 for (CH ₃ CN)(CH ₃ OH)H ⁺ 5.39, 99.4, 99.4 for CH ₃ CNH ⁺ 6.61, 34.3, 35.5 for CH ₃ OH
(CH ₃ CN)(CH ₃ CH ₂ OH)H ⁺	36, 51, 88, 125, 207, 251, 328, 329, 408, 512, 783, 790, 900, 950, 970, 1014, 1015, 1066, 1157, 1223, 1268, 1396, 1418, 1419, 1446, 1456, 1473, 1664, 2144, 2159, 2937, 2943, 2991, 3019, 3039, 3039, 3040, 3073, 3455
CH ₃ CNH ⁺	322, 322, 541, 541, 866, 1008, 1008, 1362, 1394, 1394, 2183, 2927, 3029, 3029, 3486
CH ₃ CH ₂ OH	225, 279, 401, 794, 871, 1009, 1058, 1140, 1214, 1248, 1362, 1404, 1445, 1461, 1490, 2896, 2930, 2939, 3014, 3026, 3546
transition state (common)	265, 325, 326, 404, 527, 587, 792, 827, 989, 883, 1011, 1011, 1062, 1103, 1149, 1219, 1258, 1366, 1368, 1400, 1406, 1406, 1446, 1459, 1481, 2164, 2923, 2934, 2935, 2965, 2984, 3017, 3033, 3034, 3034, 3501
transition state (vanishing) ^b	36, 51, 88, 125
α values	0.27, 0.31, 0.25, 0.25
rotational constant for rotor (GHz)	19.7
moment of inertia (10 ⁻⁴⁷ kg m ⁻²)	42.6, 1030, 1050 for (CH ₃ CN)(CH ₃ CH ₂ OH)H ⁺ 5.39, 99.4, 99.4 for CH ₃ CNH ⁺ 24.2, 89.3, 103 for CH ₃ CH ₂ OH
(CH ₃ CN)(CH ₃ CH ₂ CH ₂ OH)H ⁺	33, 40, 86, 111, 121, 186, 225, 286, 328, 329, 434, 511, 746, 825, 864, 893, 903, 969, 1013, 1015, 1017, 1087, 1158, 1204, 1247, 1279, 1310, 1374, 1375, 1395, 1419, 1419, 1456, 1461, 1466, 1472, 1663, 2146, 2193, 2926, 2936, 2943, 2979, 2989, 3019, 3032, 3040, 3040, 3063, 3452
CH ₃ CH ₂ CH ₂ OH ₂ ⁺	123, 196, 230, 245, 399, 724, 734, 756, 866, 887, 955, 1009, 1131, 1171, 1235, 1289, 1302, 1366, 1401, 1466, 1467, 1475, 1482, 1614, 2940, 2950, 2995, 3006, 3038, 3049, 3084, 3374, 3470
CH ₃ CN	311, 311, 886, 1020, 1020, 1379, 1437, 1437, 2091, 2942, 3032, 3032
transition state (common)	122, 210, 265, 319, 320, 417, 561, 617, 740, 791, 865, 895, 928, 1017, 1018, 1048, 1145, 1188, 1241, 1284, 1306, 1371, 1377, 1398, 1428, 1428, 1461, 1464, 1470, 1477, 1638, 2118, 2567, 2938, 2943, 2966, 2993, 3013, 3034, 3036, 3036, 3058, 3218, 3461
transition state (vanishing) ^b	33, 40, 86, 111
α values	0.13, 0.09, 0.03, 0.08
rotational constant for rotor (GHz)	10.6
moment of inertia (10 ⁻⁴⁷ kg m ⁻²)	78.8, 1460, 1510 for (CH ₃ CN)(CH ₃ CH ₂ CH ₂ OH)H ⁺ 34.4, 235, 252 for CH ₃ CH ₂ CH ₂ OH ₂ ⁺ 5.29, 92.9, 92.9 for CH ₃ CN
(CH ₃ CN)((CH ₃) ₂ CHOH)H ⁺	6, 36, 47, 89, 116, 197, 219, 265, 329, 330, 352, 388, 449, 510, 706, 875, 898, 916, 920, 954, 1014, 1015, 1064, 1109, 1175, 1235, 1308, 1355, 1374, 1395, 1396, 1419, 1420, 1438, 1446, 1456, 1464, 1671, 2141, 2348, 2930, 2937, 2943, 2980, 3015, 3026, 3031, 3036, 3039, 3040, 3445
(CH ₃) ₂ CHOH ₂ ⁺	184, 232, 268, 346, 354, 426, 607, 742, 857, 894, 919, 926, 1082, 1157, 1196, 1313, 1351, 1393, 1402, 1443, 1454, 1465, 1471, 1614, 2937, 2941, 3019, 3024, 3029, 3039, 3050, 3370, 3469
CH ₃ CN	311, 311, 886, 1020, 1020, 1379, 1437, 1437, 2091, 2942, 3032, 3032
transition state (common)	225, 267, 320, 320, 347, 349, 371, 438, 657, 809, 887, 892, 907, 936, 995, 1017, 1018, 1095, 1166, 1215, 1311, 1353, 1377, 1394, 1399, 1428, 1428, 1440, 1450, 1461, 1468, 1642, 2116, 2859, 2934, 2940, 2943, 3000, 3020, 3027, 3035, 3035, 3036
transition state (vanishing) ^b	36, 47, 89, 116
α values	0.13, 0.17, 0.05, 0.09
rotational constant for rotor (GHz)	7.0
moment of inertia (10 ⁻⁴⁷ kg m ⁻²)	120, 1130, 1200 for (CH ₃ CN)((CH ₃) ₂ CHOH)H ⁺ 1080, 1090, 1870 for (CH ₃) ₂ CHOH ₂ ⁺ 5.29, 92.9, 92.9 for CH ₃ CN

^a Vibrational frequencies calculated at the MP2/6-31+G(d) level of theory, scaled by 0.9434. ^b Frequencies which are varied according to eq 6.

(for CH₃–CH₃, α = 0.92 Å⁻¹)³⁰ or in the dissociation of bromobenzene ions (α = 1 and 2 Å⁻¹).²⁴

The bottleneck of the dissociation reaction was found to move to lower values of *R* as the internal energy of the ion increased as is expected from variational TST. The log *k*(*E*) versus *E* curves (Figure 2) for the two propanol-containing complexes show that the rate constants accessible on the metastable time frame (10⁴–10⁶ s⁻¹) corresponding to the dissociation of metastable ions in our VG ZAB mass spectrometer occur over an internal energy range of 2.1–2.6 eV. The internal energy range for the methanol and ethanol systems is narrower, 1.40–

1.47 eV for methanol and 1.52–1.70 eV for ethanol, due to the smaller density of states in these latter two systems. For (CH₃–CN)(CH₃CH₂CH₂OH)H⁺, *R*^{*} remained constant at 8.5 Å, while for the other three systems, a small range of *R*^{*} values was observed. For (CH₃CN)(CH₃OH)H⁺ and (CH₃CN)(CH₃CH₂–OH)H⁺, *R*^{*} occurred within the respective ranges of 6.5–7.5 and 6.0–7.0 Å, while for (CH₃CN)((CH₃)₂CHOH)H⁺, the *R*^{*} value ranged from 7.0 to 7.5 Å.

These values of *R*^{*} are consistent with the calculated α values. The larger α values for (CH₃CN)(CH₃OH)H⁺ and (CH₃CN)–(CH₃CH₂OH)H⁺ mean that the frequencies of the vanishing

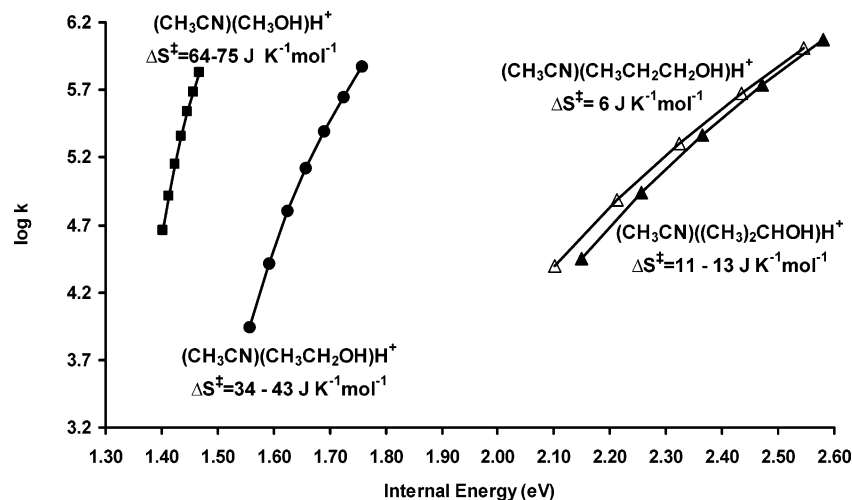


Figure 2. Calculated $\log k(E)$ vs E curves for the dissociation of the four proton-bound complexes.

vibrational modes decrease rapidly with increasing R , pulling the variational transition state closer to the equilibrium configuration than in the case of $(\text{CH}_3\text{CN})(\text{CH}_3\text{CH}_2\text{CH}_2\text{OH})\text{H}^+$ and $(\text{CH}_3\text{CN})((\text{CH}_3)_2\text{CHOH})\text{H}^+$. Larger decreases in the vanishing mode frequencies for the smaller complexes at the transition state result in larger entropies of activation. The values of ΔS^\ddagger ranged from 64 to 75 $\text{J K}^{-1} \text{mol}^{-1}$ for $(\text{CH}_3\text{CN})(\text{CH}_3\text{OH})\text{H}^+$, 34–43 $\text{J K}^{-1} \text{mol}^{-1}$ for $(\text{CH}_3\text{CN})(\text{CH}_3\text{CH}_2\text{OH})\text{H}^+$, 6 $\text{J K}^{-1} \text{mol}^{-1}$ for $(\text{CH}_3\text{CN})(\text{CH}_3\text{CH}_2\text{CH}_2\text{OH})\text{H}^+$, and 11–13 $\text{J K}^{-1} \text{mol}^{-1}$ for $(\text{CH}_3\text{CN})((\text{CH}_3)_2\text{CHOH})\text{H}^+$. The ranges in ΔS^\ddagger stem from the ranges in R^* obtained over the internal energy window of interest.

The nonvanishing, or common, vibrational modes can also contribute to the entropy of activation, albeit on a smaller scale. When the geometric parameters (and related vibrational frequencies) of the complexes are compared to those of the free products (Figure 3), differences are observed between the two smaller complexes $(\text{CH}_3\text{CN})(\text{CH}_3\text{OH})\text{H}^+$ and $(\text{CH}_3\text{CN})(\text{CH}_3\text{CH}_2\text{OH})\text{H}^+$ and the two propanol-containing complexes. The proton in $(\text{CH}_3\text{CN})(\text{CH}_3\text{OH})\text{H}^+$ and in $(\text{CH}_3\text{CN})(\text{CH}_3\text{CH}_2\text{OH})\text{H}^+$ lies closer to the alcohol moiety with O–H and N–H bond lengths of 1.075 and 1.474 Å in $(\text{CH}_3\text{CN})(\text{CH}_3\text{OH})\text{H}^+$ and 1.060 and 1.519 Å, respectively, in $(\text{CH}_3\text{CN})(\text{CH}_3\text{CH}_2\text{OH})\text{H}^+$ despite acetonitrile having a significantly higher proton affinity ($\Delta\text{PA} = 24.9 \text{ kJ mol}^{-1}$) than methanol and a slightly higher proton affinity than ethanol ($\Delta\text{PA} = 2.8 \text{ kJ mol}^{-1}$).³¹ It might have been expected that the proton should lie closer to the species with the higher proton affinity. Fridgen et al.³² attribute the position of the proton in the two complexes to the ion–dipole interaction. The dipole moments of acetonitrile and methanol are 3.92 and 1.70 D, respectively, and the minimum energy structure of the complex has a calculated dipole moment of 1.60 D. They found that by stretching and freezing the O–H bond at 1.5 Å the N–H bond shortens to 1.094 Å, the energy of the system increases by 22 kJ mol^{-1} , and the value of the dipole moment increases to 3.41 D. They proposed that increasing the magnitude of the ion–dipole interaction in the complex (by associating the proton with the lower dipole moment moiety) would contribute to lowering the energy of the complex since this would lower its overall dipole moment. Consistent with this explanation, the proton resides nearer the higher PA (and lower dipole moment) moiety in the two propanol-containing complexes.

In $(\text{CH}_3\text{CN})(\text{CH}_3\text{OH})\text{H}^+$, the C–C and C–N bonds of free acetonitrile are 1.451 and 1.159 Å; these bond lengths increase

mildly to 1.459 and 1.173 Å in the proton-bound complex. The bonds have similar lengths in $(\text{CH}_3\text{CN})(\text{CH}_3\text{CH}_2\text{OH})\text{H}^+$ since both complexes dissociate to form CH_3CNH^+ and their respective alcohol. The trend is reversed in the propanol-containing complexes with the C–C and C–N bonds elongating upon dissociation. In $(\text{CH}_3\text{CN})(\text{CH}_3\text{OH})\text{H}^+$, the C–O bond length goes from 1.487 Å in the complex to 1.431 Å in the free product while a more significant change is observed in the C–O bond length of $(\text{CH}_3\text{CN})(\text{CH}_3\text{CH}_2\text{OH})\text{H}^+$. In this pair, the bond length decreases from 1.508 Å in the complex to 1.437 Å in the free moiety. Even with such large bond length changes, however, the $\angle\text{HOC}$ angle in methanol decreases by only 3° (from 112° to 109° upon dissociation) and the $\angle\text{OCC}$ angle increases from 106° to 112°. Similarly in the ethanol complex, the $\angle\text{HOC}$ angle decreases from 111° to 109° while the $\angle\text{OCC}$ angle increases from 106° to 107° upon dissociation. The reverse trend is observed in the propanol pairs where the C–O bond length increases upon dissociation (Figure 3), the $\angle\text{HOC}$ angles increase upon dissociation (by 1° and 2° for $(\text{CH}_3\text{CN})(\text{CH}_3\text{CH}_2\text{CH}_2\text{OH})\text{H}^+$ and $(\text{CH}_3\text{CN})((\text{CH}_3)_2\text{CHOH})\text{H}^+$, respectively), and the $\angle\text{OCC}$ angles decrease (by 2° in each case). Such minor geometry changes result in only small changes in the vibrational frequency of each common mode during the dissociation. Indeed, if the vibrational frequencies of the vanishing modes are fixed at their respective values in the equilibrium complexes, the calculated ΔS^\ddagger values are very small in magnitude, with some values being tight.

The values of ΔS^\ddagger for the bond cleavage reactions are clearly different from the values calculated for ΔS . Thermodynamic entropy changes of 92, 103, 91, and 101 $\text{J K}^{-1} \text{mol}^{-1}$ were found for $(\text{CH}_3\text{CN})(\text{CH}_3\text{OH})\text{H}^+$, $(\text{CH}_3\text{CN})(\text{CH}_3\text{CH}_2\text{OH})\text{H}^+$, $(\text{CH}_3\text{CN})(\text{CH}_3\text{CH}_2\text{CH}_2\text{OH})\text{H}^+$, and $(\text{CH}_3\text{CN})((\text{CH}_3)_2\text{CHOH})\text{H}^+$, respectively (Table 2). Positive entropy changes were observed in the translational and rotational entropy of each proton-bound system, while a negative entropy change was found in the vibrational entropy due to the loss of six low vibrational frequency modes in the products. There is a definite trend in the ΔS^\ddagger values, with the values decreasing as the alcohol side chain lengthens, due to the migration of the variational transition state farther away from the reactant complex (see above). This trend is absent in the thermodynamic ΔS . There is a greater absolute change in magnitude in ΔS^\ddagger in going from $X = \text{CH}_3$ to $X = \text{CH}_3\text{CH}_2\text{CH}_2$ ($\sim 70 \text{ J K}^{-1} \text{mol}^{-1}$) than there is variation between the thermodynamic ΔS (12 $\text{J K}^{-1} \text{mol}^{-1}$) in addition to greater relative changes (a factor of ~ 11 for ΔS^\ddagger and 1.1 for ΔS) (Table 2). In

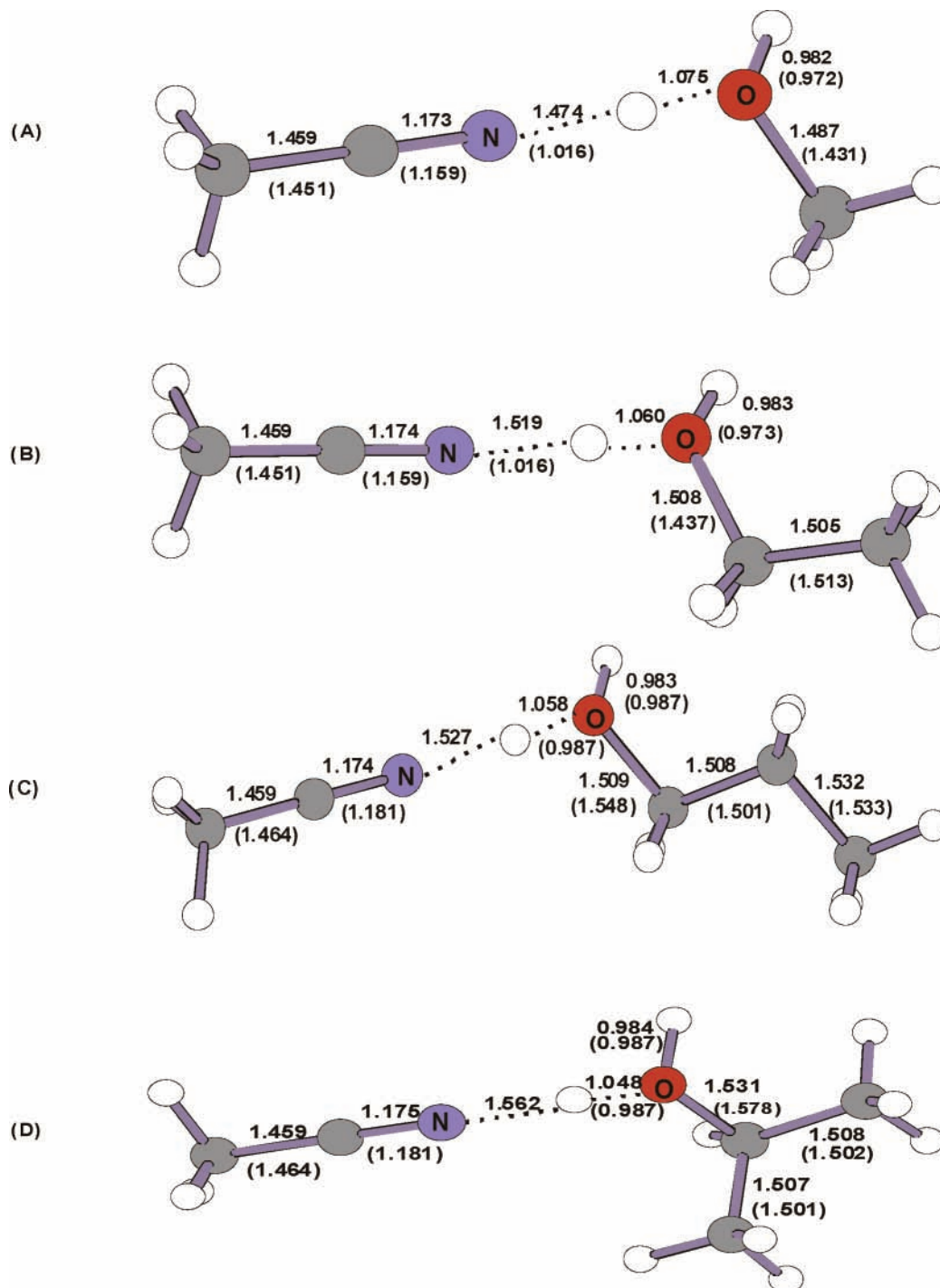


Figure 3. Selected optimized geometric parameters for the four proton-bound complexes obtained at the MP2/6-31+G(d) level of theory. Values corresponding to the free products are in parentheses.

TABLE 2: Thermodynamic and Activation Entropies for a Series of Acetonitrile–Alcohol Proton-Bound Pairs^a

proton-bound dimer	ΔS^\ddagger ^b	ΔS	ΔS_{trans}	ΔS_{rot}	ΔS_{vib}
$(\text{CH}_3\text{CN})(\text{CH}_3\text{OH})\text{H}^+$	64–75	92	159	65	–132
$(\text{CH}_3\text{CN})(\text{CH}_3\text{CH}_2\text{OH})\text{H}^+$	34–43	103	162	74	–133
$(\text{CH}_3\text{CN})(\text{CH}_3\text{CH}_2\text{CH}_2\text{OH})\text{H}^+$	6	91	163	77	–149
$(\text{CH}_3\text{CN})((\text{CH}_3)_2\text{CHOH})\text{H}^+$	11–13	101	163	78	–140

^a In $\text{J K}^{-1} \text{mol}^{-1}$ at 600 K. ^b Estimated uncertainty, $\pm 3 \text{ J K}^{-1} \text{mol}^{-1}$.

light of these different trends, it may be wise to be careful in assigning $\Delta(\Delta S^\ddagger) = \Delta(\Delta S)$ in the competitive dissociation reactions of proton-bound pairs, even when the two components of the complex are structurally related.

4. Conclusions

The entropies of activation for the dissociation of a series of acetonitrile–alcohol proton-bound pairs $(\text{CH}_3\text{CN})(\text{CH}_3\text{OH})\text{H}^+$, $(\text{CH}_3\text{CN})(\text{CH}_3\text{CH}_2\text{OH})\text{H}^+$, $(\text{CH}_3\text{CN})(\text{CH}_3\text{CH}_2\text{CH}_2\text{OH})\text{H}^+$, and $(\text{CH}_3\text{CN})((\text{CH}_3)_2\text{CHOH})\text{H}^+$ were determined with microcanonical variational transition state theory. The values were found to correlate with the changes that occur in the geometries of the complexes upon dissociation, greater changes yielding greater ΔS^\ddagger values. It was also found that the changes in ΔS^\ddagger in going from $(\text{CH}_3\text{CN})(\text{CH}_3\text{OH})\text{H}^+$ to $(\text{CH}_3\text{CN})((\text{CH}_3)_2\text{CHOH})\text{H}^+$ were not quantitatively mirrored in the thermodynamic ΔS values for the four dissociation reactions.

Acknowledgment. P.M.M. thanks the Natural Sciences and Engineering Research Council of Canada for continued funding. The authors thank a reviewer for many helpful comments. Dedicated to Tomas Baer, mentor and colleague, for his many outstanding contributions to gas-phase ion chemistry.

References and Notes

- (1) Dunbar, R. C.; McMahon, T. B. *Science* **1998**, *279*, 194.
- (2) Dunbar, R. C. *Mass Spectrom. Rev.* **2004**, *23*, 127.
- (3) Baer, T. *Adv. Chem. Phys.* **1986**, *64*, 111.
- (4) Baer, T.; Mayer, P. M. *J. Am. Soc. Mass Spectrom.* **1997**, *8*, 103.
- (5) Armentout, P. B.; Rodgers, M. T. *J. Phys. Chem. A* **2000**, *104*, 2238.
- (6) Laskin, J.; Bailey, T. H.; Futrell, J. H. *Int. J. Mass Spectrom.* **2004**, *234*, 89.
- (7) McLuckey, S. A.; Cameron, D.; Cooks, R. G. *J. Am. Chem. Soc.* **1981**, *130*, 1313.
- (8) Cheng, X.; Wu, Z.; Fenselau, C. *J. Am. Chem. Soc.* **1993**, *115*, 4844.
- (9) Wu, Z.; Fenselau, C. *Rapid Commun. Mass Spectrom.* **1994**, *8*, 777.
- (10) Cerda, B. A.; Wesdemiotis, C. *J. Am. Chem. Soc.* **1996**, *118*, 11884.
- (11) Cerda, B. A.; Hoyau, S.; Ohanessian, G.; Wesdemiotis, C. *J. Am. Chem. Soc.* **1998**, *120*, 2437.
- (12) Cerda, B. A.; Wesdemiotis, C. *Int. J. Mass Spectrom.* **1999**, *185/186/187*, 107.
- (13) Zheng, X.; Cooks, R. G. *J. Phys. Chem. A* **2002**, *106*, 9939.
- (14) Hache, J. J.; Laskin, J.; Futrell, J. H. *J. Phys. Chem. A* **2002**, *106*, 12051.
- (15) Klotz, C. E. *Z. Phys. D* **1991**, *21*, 335.
- (16) Drahos, L.; Vekey, K. *J. Mass Spectrom.* **2003**, *38*, 1025.
- (17) Ervin, K. M. *J. Am. Soc. Mass Spectrom.* **2002**, *13*, 435.
- (18) Ochran, R. A.; Mayer, P. M. *Eur. J. Mass Spectrom.* **2001**, *7*, 267.
- (19) Frisch, M. J.; Trucks, G. W.; Schlegel, H. B.; Scuseria, G. E.; Robb, M. A.; Cheeseman, J. R.; Zakrzewski, V. G.; Montgomery, J. A., Jr.; Stratmann, R. E.; Burant, J. C.; Dapprich, S.; Millam, J. M.; Daniels, A. D.; Kudin, K. N.; Strain, M. C.; Farkas, O.; Tomasi, J.; Barone, V.; Cossi, M.; Cammi, R.; Mennucci, B.; Pomelli, C.; Adamo, C.; Clifford, S.; Ochterski, J.; Petersson, G. A.; Ayala, P. Y.; Cui, Q.; Morokuma, K.; Malick, D. K.; Rabuck, A. D.; Raghavachari, K.; Foresman, J. B.; Cioslowski, J.; Ortiz, J. V.; Stefanov, B. B.; Liu, G.; Liashenko, A.; Piskorz, P.; Komaromi, I.; Gomperts, R.; Martin, R. L.; Fox, D. J.; Keith, T.; Al-Laham, M. A.; Peng, C. Y.; Nanayakkara, A.; Gonzalez, C.; Challacombe, M.; Gill, P. M. W.; Johnson, B. G.; Chen, W.; Wong, M. W.; Andres, J. L.; Head-Gordon, M.; Replogle, E. S.; Pople, J. A. *Gaussian 98*, revision A.7; Gaussian, Inc.: Pittsburgh, PA, 1998.
- (20) Scott, A. P.; Radom, L. *J. Phys. Chem.* **1996**, *100*, 16502.
- (21) Baer, T.; Hase, W. L. *Unimolecular Reaction Dynamics, Theory and Experiments*; Oxford University Press: New York, 1996.
- (22) Pechukas, P. *Annu. Rev. Phys. Chem.* **1981**, *32*, 159.
- (23) Truhlar, D. G.; Garrett, B. C. *Acc. Chem. Res.* **1980**, *13*, 440.
- (24) Lifshitz, C.; Louage, F.; Aviyente, V.; Song, K. *J. Phys. Chem.* **1991**, *95*, 9298.
- (25) Beyer, T.; Swinehart, D. R. *ACM Commun.* **1973**, *16*, 379.
- (26) Hase, W. L. *J. Chem. Phys.* **1972**, *57*, 730.
- (27) Quack, M.; Troe, J. *Ber. Bunsen-Ges. Phys. Chem.* **1974**, *78*, 240.
- (28) Mayer, P. M.; Keister, J. W.; Baer, T.; Evans, M.; Ng, C. Y.; Hsu, C.-W. *J. Phys. Chem. A* **1997**, *101*, 1270.
- (29) Hase, W. L. *Chem. Phys. Lett.* **1987**, *139*, 389.
- (30) Hase, W. L. *J. Chem. Phys.* **1976**, *64*, 2442.
- (31) Linstrom, P. J.; Mallard, W. G. *NIST Chemistry WebBook, NIST Standard Reference Database Number 69*; National Institute of Standards and Technology: Gaithersburg, MD, March 2003.
- (32) Fridgen, T. D.; Keller, J. D.; McMahon, T. B. *J. Phys. Chem. A* **2001**, *105*, 3816.